Assessing the Contribution of the Lowest Triplet State to the Near-UV Absorption Spectrum of HOCl

Rhett James Barnes and Amitabha Sinha*

Department of Chemistry and Biochemistry, University of California—San Diego, 9500 Gilman Drive, La Jolla, California 92093-0314

Hope A. Michelsen

AER, Inc., 2682 Bishop Dr., Suite 120, San Ramon, California 94583

Received: September 1, 1998

The near-UV absorption spectrum of HOCl is examined using laser induced fluorescence to monitor OH fragments resulting from photodissociation. The measured variation in OH photofragment yields along with an analysis of their Doppler line shapes reveals the presence of a weak absorption feature centered at 380 nm arising from excitation to the lowest excited triplet electronic state of HOCl. Although the peak absorption cross section for the band is modest, $\sigma(380\text{ nm}) = 4 \times 10^{-21}$ cm^2 , its long-wavelength tail extends down to 480 nm. Present estimates suggest that as a result of absorption by the triplet state, the instantaneous photochemical lifetime of stratospheric HOCl will be shortened by 10−20% and the average abundance reduced by 11−12% relative to previous estimates.

Introduction

Hypochlorous acid, HOCl, is an atmospherically important chlorine-containing molecule which is formed predominantly in the stratosphere by the gas phase reaction

$$HO_2 + ClO \rightarrow HOCl + O_2 \quad (1)$$

HOCl plays a particularly important role in the conversion of relatively photochemically stable chlorine reservoir species, HCl and $ClONO_2$, to more reactive species via the heterogeneous reactions

$$ClONO_2 + H_2O \rightarrow HOCl + HNO_3 \quad (2)$$

$$HCl + HOCl \rightarrow Cl_2 + H_2O \quad (3)$$

These reactions proceed rapidly at the low temperatures that occur during the polar nights and initiate the catalytic destruction of ozone in the Antarctic and Arctic spring.[1] Since photodissociation is an important removal mechanism for atmospheric HOCl, there has been great interest in characterizing its near-UV absorption spectrum and understanding its photochemistry.[2−5] Previous studies on HOCl have primarily focused on excitation to singlet electronic excited states, which comprise the dominant absorption features occurring in the near-UV region of the spectrum between 200 and 380 nm. However, as the chlorine atom is relatively heavy, contributions from transitions to excited triplet electronic states which can potentially borrow intensity from nearby "bright" singlet state(s) through spin−orbit interaction also need to be carefully examined. Of the various possible triplet states in HOCl, absorption by the first excited triplet state is expected to be most important under atmospheric conditions since its absorption profile is situated at substantially longer wavelength compared to that of the first excited singlet state. The triplet absorption is thus expected to be preferentially enhanced by the solar actinic flux, which peaks in the visible region of the spectrum.

In the present work we investigate the triplet absorption band of HOCl using laser-induced fluorescence (LIF) detection in conjunction with sub-Doppler spectroscopy. The dependence of the relative OH photofragment yield on photolysis wavelength allows us to map out the absorption cross section of HOCl from ∼290 nm to 500 nm. In addition, an analysis of the OH Doppler line shape provides information on the orientation of the electronic transition moment and hence the symmetry of the excited electronic state(s) accessed through photoabsorption. Our results indicate that the absorption arising from excitation to the first excited triplet sate of HOCl is centered at ∼380 nm and appears as a shoulder on the red edge of the much stronger $1^1A'' \leftarrow X^1A'$ band system. Although the peak absorption cross section of this triplet absorption is modest (∼4×10^{-21} cm^2 at 380 nm), the long-wavelength tail of the band extends to 480 nm. Hence, as in the case of HOBr,[6] absorption by the first excited triplet state of HOCl makes a nonnegligible contribution to the overall atmospheric photochemical activity of the molecule.

Experimental Section

The experiments on HOCl were carried out using the same apparatus that was used in our earlier work on HOBr.[6] We generate HOCl by flowing water vapor and Cl_2 through two separate ports located at one end of a glass column packed with a mixture of yellow HgO powder and 6 mm diameter glass beads. The beads allow loose packing of the HgO and thus ensure uniform flow of the reagent gases through the column. The other end of the column is connected to the glass photolysis cell, and the mixture of reactants and HOCl products continuously flow into the cell. The cell is evacuated by a partially throttled mechanical vacuum pump resulting in a total pressure in the cell of ∼80 mTorr. All components coming in contact

10.1021/jp9835869 CCC: $15.00
Published on Web 10/16/1998

with the reagents prior to entering the cell are made of either glass or Teflon in order to avoid catalytic loss of HOCl on metal surfaces. Under typical flow conditions, the column is able to generate sufficient yields of HOCl to last several days before requiring refilling.

Photolysis radiation required for these measurements is generated by a combination of methods. For accessing the wavelength region from 440 to 500 nm, the signal beam from an optical parametric oscillator (OPO, Spectra Physics MOPO-730), which is pumped by the third harmonic of a Nd:YAG laser (Spectra Physics GCR-270), is used. The OPO laser provides continuously tunable radiation over this entire wavelength region with a bandwidth of $\sim$0.3 cm^{-1} and pulse energies ranging from 10 to 60 mJ. Photolysis wavelength in the 396−416 nm range is generated by stimulated Raman shifting the output of a Nd:YAG laser-pumped dye laser in a high-pressure cell containing either H_2 or methane (150−200 psig). Typically the second anti-Stokes-shifted output is required, and it is separated from the other wavelengths present using a Pellin-Broca prism assembly. The photolysis beam is passed through a 3× telescope to reduce its diameter and is subsequently directed into the photolysis cell through a set of baffled side arms. Nominally, the photolysis beam travels collinearly relative to the probe laser in a counter-propagating fashion. However, for some of the Doppler profile measurements we have also used an orthogonal geometry with the probe and photolysis lasers traveling perpendicular to each other. We typically keep the diameter of the probe laser beam substantially larger than that of the photolysis beam in order to ensure detection of all the OH fragments with minimal loss due to diffusion out of the viewing region.

The OH photofragments are probed via the A−X transition at $\sim$308 nm using LIF. Radiation in this wavelength region is generated by frequency doubling the output of a second Nd:YAG laser (Continuum NY81-20) pumped dye laser (Continuum ND60). The probe laser has a bandwidth of $\sim$0.12 cm^{-1} in the UV. Both photolysis and probe lasers are operated at 20 Hz with the time delay between them variable from 20 ns to 1.5 μs depending on the particular measurement. For detection of the nascent OH fragment Doppler profiles, the time delay is typically set between 20 and 30 ns to prevent interference from collisions. In determining the absolute cross section of the band, we compare the relative yield of OH fragments generated at various photolysis wavelengths with that from the photolysis of HOCl at 355 nm where its absorption cross section is known from the work of Burkholder.[2a] For these cross-section measurements, the pressure in the cell is increased from its nominal value of 80 mTorr to about 700 mTorr by adding N_2 buffer gas and the time delay between the photolysis and probe lasers is increased to about 1 μs in order to ensure thermalization of the nascent OH rotational state distribution.

The fluorescence excited by the probe laser is imaged onto a photomultiplier tube (EMI 9635QB) using an *f*/1 lens system, and a gated integrator captures the resulting signal for subsequent storage on a personal computer. A colored glass filter (Corning 7-54) and a 310 nm interference filter (Acton Research) are used to reduce scattered light. In addition, two sharp-cutoff filters are used to reject wavelengths longer than 340 nm. The photolysis laser energy is measured as the beam exits the photolysis cell using a volume absorber laser power meter (Ophir), and the probe laser energy is monitored using a photodiode. The power readings for both lasers are simultaneously recorded along with the OH fluorescence signal for purposes of normalization.

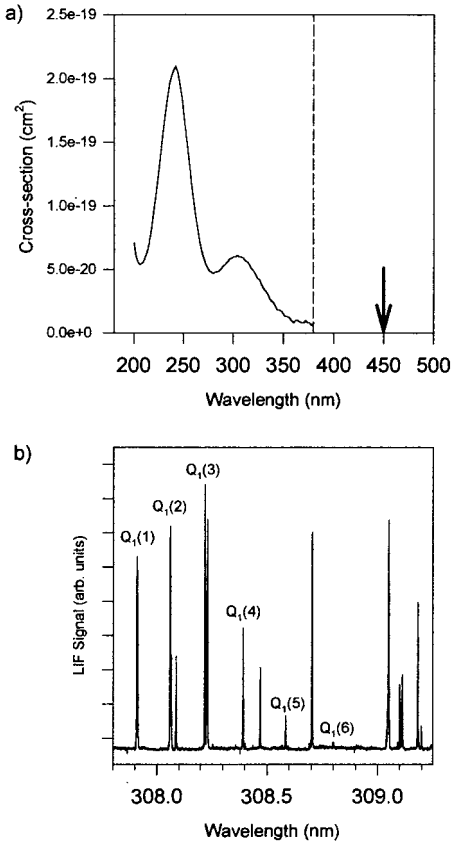

Figure 1. (a) HOCl UV cross section data from Burkholder (ref 2a). The dashed line shows the long-wavelength cutoff of these data. (b) Nascent OH LIF signal detected from 450 nm photolysis of HOCl

Results and Discussion

The first issue we address is the wavelength region over which the near-UV absorption spectrum of HOCl extends. Figure 1a shows the absorption spectrum of HOCl reported by Burkholder over the 200−380 nm range.[2a] Presumably the reason that the spectrum does not extend beyond 380 nm is due to the inability of the direct absorption technique to detect weaker absorption features beyond this point. Figure 1a gives the impression that access to excited electronic states of HOCl ceases beyond 380 nm. Using laser-induced fluorescence, however, we are able to detect the production of OH fragments from HOCl for photolysis wavelengths as long as 480 nm. As an example, Figure 1b displays the nascent OH LIF spectrum following photolysis at 450 nm.

In the present study we have not attempted to characterize the HOCl absorption spectrum continuously over the entire range from 380 to 500 nm but have recorded the relative yield of OH photofragments at several discrete points over this region. Figure 2a displays the cross section data obtained by monitoring signal from the OH(v''=0,N=2,$^2\Pi_{3/2}$) state under conditions where the nascent fragment rotational state distribution has been thermalized. In order to relate these measurements to an absolute cross section, we take the ratio of thermalized OH(v''=0,N=2,$^2\Pi_{3/2}$) yield at each of the indicated wavelengths with that obtained from the photolysis of HOCl at a reference wavelength corresponding to 355 nm. The choice of reference wavelength is dictated by convenience, 355 nm being the third harmonic of the Nd:YAG laser, and by the fact that it falls within the spectral range covered by the Burkholder measurements and hence allows direct calibration with his absorption cross-section data. As a further internal consistency check, we have also

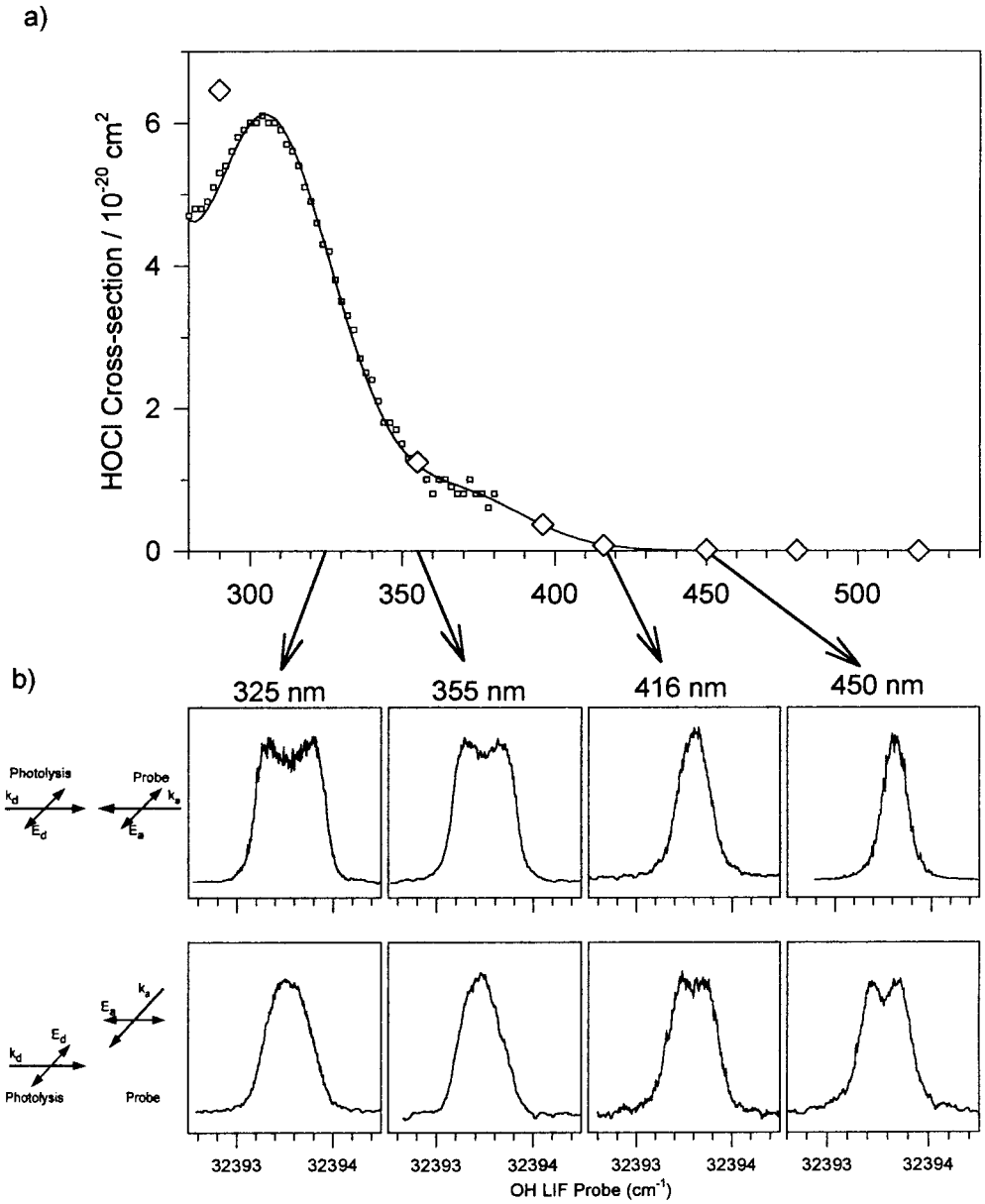

Figure 2. (a) Composite spectrum showing Burkholder data (small squares) ref 2a, data from relative OH yield measurements (large diamonds), and a best fit line through the combined data set. (b) OH(v''=0,N=2,$^2\Pi_{3/2}$) Doppler line shapes resulting from photolysis of HOCl at various wavelengths. Doppler profiles in a given row are recorded using the same experimental geometry, identified at the left.

TABLE 1: Measured Absorption Cross Sections

wavelength (nm)	cross section (cm^2)[a]
290	6.46×10^{-20}
355	1.25×10^{-20}
396	3.70×10^{-21}
416	7.55×10^{-22}
450	1.78×10^{-22}
480	5.52×10^{-23}
530	0

[a] Absolute cross-section data at 355 nm from Burkholder is used for normalization.

compared the OH yield from HOCl photolysis at 355 nm with that resulting from 290 nm photolysis and find that the ratio of the yields agrees with the ratio of the reported absorption cross sections for these wavelengths. Table 1 summarizes the measured absorption cross-section data. As Figure 2a shows, connecting the new data points with those from the previous measurements of Burkholder reveals the presence of a slight shoulder in the near-UV spectrum arising from the presence of an absorption feature centered around 380 nm. In order to better quantify the strength of the new absorption band, we have deconvoluted the contributions of the various absorption features that comprise the near-UV absorption spectrum of HOCl using three functions centered at 240, 325, and 380 nm having the form

$$\sigma(v) = Av \exp[-(v-B)^2/C^2] \qquad (4)$$

with the coefficients A, B, and C being treated as adjustable parameters. The results of the deconvolution are shown in Figure 3, and the resulting best fit parameters are given in Table 2. We provide arguments below that strongly suggest that the weak feature at 380 nm is due to excitation to the lowest triplet state of HOCl.

In addition to characterizing the variation in absorption cross section with wavelength, we have also used sub-Doppler spectroscopy to examine how the Doppler profiles of the nascent OH photofragments change with excitation wavelength and relative polarization/propagation direction of the photolysis and

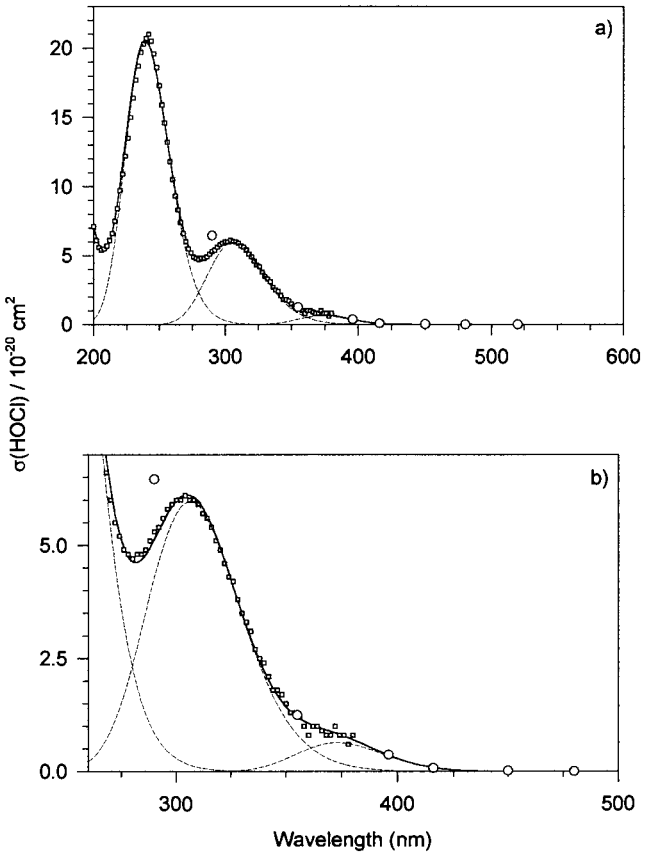

Figure 3. (a) Deconvolution of near-UV absorption data of HOCl into their three contributing absorption features. The square data points are from ref 2a; circles are from the present OH relative yield measurements. The solid line is the composite fit, and the dashed lines correspond to contributions from individual bands (see Table 2). (b) Detailed look at the near-visible spectral region.

TABLE 2: Best Fit Parameters Resulting from Deconvolution of HOCl UV/Vis Data[a]

	A_n	B_n	C_n
$n = 1$	7.125	26736.5	1383.43
$n = 2$	55.007	32491.8	2250.38
$n = 3$	147.161	41564.9	2899.15

[a] The functional form used for the fit is

$$\sigma(\upsilon) = 10^{-21}\left\{\left[244.333\exp\left(-0.5\left(\frac{\upsilon - 58126.6}{5088.82}\right)^2\right)\right] + \sum_{n=1}^{3}\left[\left(\frac{A_n}{30000}\right)\upsilon\exp\left(-0.5\left(\frac{\upsilon - B_n}{C_n}\right)^2\right)\right]\right\}$$

The above equation consists of three functions of the form given by eq 4 (those inside the summation), with an additional Gaussian function (left of the summation) to account for absorption from the tail of the third excited singlet band at wavelengths < 220 nm.

probe lasers. The procedure used in these measurements is similar to that outlined in our previous work on HOBr[6b] and allows us to ascertain the symmetry of the excited electronic state. Figure 2b displays a series of Doppler line shapes for the nascent OH(v''=0,N=2,$^2\Pi_{3/2}$) rotational state taken under two different experimental geometries for various excitation wavelengths. The observed variation in the OH Doppler profiles with excitation wavelength for the two geometries shown reveals an important trend. For photodissociation at 355 and 325 nm, the Doppler profiles for the probed OH transition display a distinct dip at line center in the collinear geometry, whereas the profile for the same transition recorded using the perpendicular configuration exhibits a maximum at line center. An analysis of these line shapes indicates that the translational anisotropy parameter $\beta = -0.40$, and thus the electronic transition moment is perpendicular to the recoil axis, consistent with excitation from the X^1A' ground state to the $1^1A''$ excited electronic state. As the excitation wavelength is gradually shifted to longer wavelength, however, one finds a reversal in the shapes of the OH Doppler profiles, and by 416 nm the Doppler profile for the collinear geometry has developed a maximum at line center, and the one at perpendicular geometry has a corresponding minimum. *This change in Doppler line shape is a clear indicator that a different excited electronic state is involved at these longer wavelengths.* An analysis of the line shapes at 416 nm suggests that β is now positive and that the transition moment is parallel to the recoil direction; the transition moment, thus, is of A′ symmetry. Since the ground electronic state is of A′ symmetry, the observation that the transition moment is of A′ symmetry then suggests that the excited electronic state accessed at these wavelengths is of A′ symmetry as well.

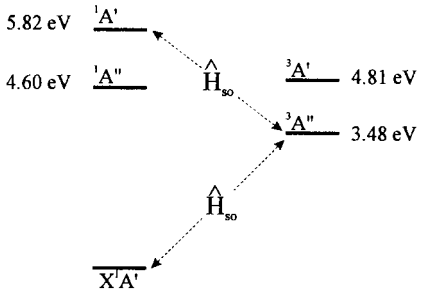

Figure 4. Predicted location of HOCl excited electronic states based on ab initio calculations of ref 4a.

In order to further narrow down the possibilities, Figure 4 summarizes the location of the lowest few excited electronic states of HOCl obtained from ab initio studies.[4] As the figure shows, there are no singlet electronic states of HOCl that can account for the observed band system at 380 nm. However, a glance at the manifold of triplet states reveals the presence of a low-lying electronic state of $^3A''$ symmetry occurring at 3.48 eV (~360 nm). We propose that the weak absorption band accessed in the current measurement corresponds to excitation to this triplet state. Although at first sight this assignment appears to be inconsistent with the measured value of β, which indicates that the transition moment points along the Cl−O bond, we note that in molecules containing heavy atoms, spin−orbit interaction can efficiently mix singlet and triplet electronic states.[7] Thus, we propose that the 380 nm band in HOCl corresponds to excitation to the lowest triplet state of A″ symmetry which, through spin−orbit interaction, borrows intensity from nearby singlet state(s) of A′ character. On the basis of energetics, the most plausible singlet states of A′ symmetry which are likely to mix with the first excited triplet state are the $2^1A'$ state located around ~240 nm and the ground electronic state, although other remote states may also contribute. Under the proposed scenario, the true eigenstates of the molecule accessed at 380 nm are appropriate admixtures of the singlet and triplet electronic states with the measured translational anisotropy parameter primarily reflecting the symmetry of the "bright" singlet state(s) contributing to the eigenstate. It is worth noting that a similar situation has been observed with regard to the photochemistry of HOBr and NOCl.[6,8] Indeed, recent high-level ab initio calculations by Minaev and Agren[9] which explicitly include spin−orbit coupling support the above conclusions. Their calculations confirm that the intensity for the $^3A''$

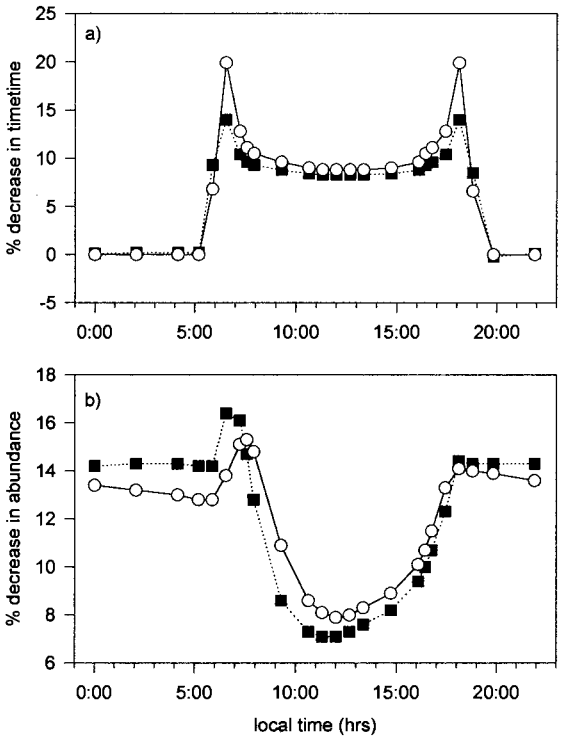

Figure 5. Influence of triplet state absorption on the instantaneous lifetime and abundance of stratospheric HOCl over a 24 h diurnal cycle. The calculations were performed for two altitudes corresponding to 17 km (circles) and 24 km (squares), a latitude of 40°, and solar conditions at equinox using the kinetic parametrs of ref 10. We define the percentage change as $[(V_{tail} - V_{no\ tail})/V_{tail}] \times 100\%$, where V_{tail} and $V_{no\ tail}$, are repectively the values obtained in the calculation with and without the triplet tail (i.e., $\lambda > 380$ nm) included. (a) Percentage change in the instantaneous lifetime arising from inclusion of triplet absorption tail. (b) Percentage change in stratospheric abundance of HOCl. The nonzero value for this quantity before sunrise results from the value attained just after sunset in the previous diurnal cycle.

← X^1A' band in HOCl arises from intensity borrowing through singlet−triplet mixing and find that the transition moment for the excitation is almost parallel to the Cl−O bond consistent with the results of the present measurements. In addition, their calculated peak absorption cross section for the band, 3.4×10^{-21} cm^2,[9] is in good agreement with the present experimental value ($\sim 4 \times 10^{-21}$ cm^2) obtained from the deconvolution, described in Figure 3, although their predicted band center, 411.5 nm, is slightly to the red of the present experimental value of 380 nm.

Because HOCl plays an important role in partitioning of inorganic chlorine in the stratosphere, absorption by the triplet state described here may contribute significantly to the distribution of chlorine species at altitudes above the tropopause. Assuming unit quantum yield for OH production from HOCl photolysis and photochemical steady state (i.e., production and loss of short-lived species are equivalent over a diurnal cycle), model calculations based on the recommended kinetic parameters[10] suggest that absorption by the portion of the triplet band previously neglected ($\lambda > 380$ nm) reduces the instantaneous photochemical lifetime of HOCl by ∼8% at midday for an altitude of 17 km, latitude of 40°, and solar conditions at equinox. The influence of this long-wavelength absorption becomes even more important with increasing solar zenith angle and results in a reduction of the HOCl lifetime by as much as 20% at sunrise and sunset (see Figure 5a).

We have also examined the influence of the triplet absorption (i.e., $\lambda > 380$ nm) on the abundance of stratospheric HOCl. Increase in latitude or solar declination or altitude shifts the average solar flux to longer wavelength and hence increases the influence of the triplet absorption band on the instantaneous lifetime. However, the influence of these parameters is rather small, and the net effect of the new absorption band, averaged over a 24 h diurnal cycle, is to cause a decrease in the HOCl abundance by 11−12%, a value that is nearly independent of latitude, altitude, and solar declination (see Figure 5b).

Thus, in summary it appears that absorption by the first excited triplet state of HOCl makes a nonnegligible contribution to atmospheric photochemistry and consequently needs to be properly accounted for when determining the photolytic lifetime of HOCl.

Acknowledgment. We thank both the National Science Foundation and the Hellman Foundation of U. C. San Diego for partial support of this research. H.A.M. was supported by NASA (NAS1-96022). We also thank Prof. R. W. Field for helpful discussion regarding spin−orbit interactions in HOCl and Prof. Kirk Peterson for providing ab initio data on the ground and first excited triplet state of HOCl prior to publication.

References and Notes

(1) Prather, M. J. *Nature* **1992**, *355*, 534.

(2) (a) Burkholder, J. B. *J. Geophys. Res.* **1993**, *98*, 2963. (b) Molina L. T.; Molina, M. J. *J. Phys. Chem.* **1978**, *82*, 2410.

(3) (a) Bell, A. J.; Pardon, P. R.; Hickman, C. G.; Frey, J. G. *J. Chem. Soc., Faraday Trans. 2* **1990**, *86*, 331. (b) Hickman, C. G.; Brickell, A.; Frey, J. G. *Chem. Phys. Lett.* **1991**, *185*, 101. (c) Hickman, C. G.; Shaw, N. S.; Crawford, M. J.; Bell, A. J.; Frey, J. G. *J. Chem. Soc., Faraday Trans. 2* **1993**, *89*, 1623.

(4) (a) Francisco, J. S.; Hand, M. R.; Williams, I. H.; *J. Phys. Chem.* **1996**, *100*, 9250. (b) Bruna, P. J.;. Hirsch, G.; Peyerimhoff, S. D.; Buenker, R. J. *Can. J. Chem.* **1979**, *57*, 1839. (c) Jaffe, R. L.; Langhoff, S. R. *J. Chem. Phys.* **1978**, *68*, 1638.

(5) (a) Guo, H. *J. Phys. Chem.* **1993**, *97*, 2602. (b) Offer A. R.; Balint-Kurti, G. G. *Chem. Phys. Lett.* **1994**, *228*, 200. (c) Offer, A. R.; Balint-Kurti, G. G. *J. Chem. Phys.* **1994**, *101*, 10416.

(6) (a) Barnes, R. J.; Lock, M.; Coleman, J.; Sinha, A. *J. Phys. Chem.* **1996**, *100*, 453. (b) Lock, M.; Barnes, R. J.; Sinha, A. *J. Phys. Chem.* **1996**, *100*, 7972.

(7) Lefebvre-Brion, H.; Field, R. W. *Perturbations in Spectra of Diatomic Molecules;* Academic Press*:* New York, 1986.

(8) Bai, Y. Y.; Ogai, A.; Qian, C. X. W.; Iwata, L.; Segal, G. A.; Reisler, H. *J. Chem. Phys.* **1989**, *90*, 3903.

(9) Minaev, B. F.; Agren, H. *J. Chem. Soc., Faraday Trans.* **1998**, *94*, 2061.

(10) (a) DeMore, W. B.; Sander, S. P.; Golden, D. M.; Hampson, R. F.; Kurylo, M. J.; Howard, C. J.; Ravishankara, A. R.; Kolb, C. E.; Molina, M. JPL Publication 97-4, 1997. (b) Michelsen, H. A., Salawitch, R. J., Gunson, M. R.; Aellig, C.; Kampfer, N.; Abbas, M. M.; Abrams, M. C.; Brown, T. L.; Chang, A. Y.; Goldman, A.; Irion, F. W.; Newchurch, M. J.; Rinsland, C. P.; Stiller, G. P.; Zander, R. *Geophys. Res. Lett.* **1996**, *23*, 2361.